JOURNAL OF MATERIALS SCIENCE 13 (1978) 178–188

High-temperature compatibility of carbon fibres with nickel

R. WARREN, C. H. ANDERSON, M. CARLSSON
Department of Engineering Metals, Chalmers University of Technology, Gothenburg, Sweden

A study has been made of the elevated temperature degradation of a number of carbon fibre types coated with nickel by a variety of methods (electroless, electrolytic, carbonyl and physical vapour deposition). At high temperatures, Ni-coated fibres undergo a transformation of structure to crystalline graphite with a consequent loss of strength and elastic modulus. Resistance to this recrystallization is related to the fibre type and structure and increases in the order HTS PAN-based, HM PAN-based, HM rayon-based. For PAN-based fibres the resistance increases with the degree of structural order and orientation. The recrystallization of HTS fibres is consistent with a simple model of dissolution and reprecipitation controlled by diffusion of carbon in nickel. To explain the higher stability of HM fibres an additional factor must be introduced. For example, their behaviour can be explained in terms of a highly stable surface layer between about 0.1 and 0.5 μm thick. Rapid recrystallization occurs when the nickel breaks through this layer e.g. by dissolution. The recrystallization was not greatly affected by the type of nickel coating but the recrystallization temperature of HM fibres was considerably reduced by a small proportion of air in the heat-treatment atmosphere. HTS fibres were not affected in this way but the fibres were severely weakened through surface attack by both air and hydrogen at temperatures well below the recrystallization temperature.

1. Introduction

Carbon fibre-reinforced nickel composites have for some time been considered as candidates for high-temperature service. Unfortunately, such composites have been found to be vulnerable to oxidation [1, 2] and to a structural degradation of the fibre at elevated temperatures [3–6]. Both processes can lead to complete loss of the favourable mechanical properties of the fibre. In the latter the characteristic, oriented fibre structure* is transformed to coarse randomly oriented graphite crystals and the process is commonly called "recrystallization". As for metallic recrystallization, the process becomes rapid over a narrow temperature range and it is possible to define a recrystallization temperature. Though it is clearly promoted by the presence of nickel, there is disagreement regarding the exact nature of the process and the role of such factors as impurities and fibre structure. High tensile strength (HTS) fibres produced form a polycacrylonitrile (PAN) precursor are observed to recrystallize rapidly between about 800 and 900° C [3, 6, 8]. Jackson and Marjoram [3] found that high modulus (HM) PAN-based fibres coated with electrolytically-deposited nickel recrystallized rapidly at about 1100° C in a vacuum of ~0.01 Pa (~10^{-4} torr). Similar results were obtained by Barnett *et al.* [4] with physically vapour-deposited (PVD) nickel on HM fibres annealed in 0.006 Pa vacuum. In contrast Barclay and Bonfield [9] observed no recrystallization in PVD-coated HM fibres annealed for up to 48 h at

*It is assumed throughout that the reader is familiar with the techniques of production and the nature of the structure and properties of carbon fibres. The subject has been reviewed e.g. by Goodhew *et al.* [7].

© *1978 Chapman and Hall Ltd. Printed in Great Britain.*

1200° C at 10^{-4} Pa. They attributed the moderate reductions in strength that they observed to dissolution of the fibre surface and suggested that recrystallization is initiated by impurities in the system. Sarian [5] found that rayon-based HM fibres in electrolytic nickel did not recrystallize during prolonged annealing at 1200° C in argon, but did so at 1250° C. Warren and Carlsson [8] have demonstrated experimentally that the observed variations in recrystallization behaviour can be related, at least partly, to differences in fibre type and structure.

In the present work an attempt has been made to identify the nature of the processes contributing to the degradation of carbon fibres in nickel and to obtain a clearer understanding of the effect of factors such as fibre structure and environment. To achieve this, experimental studies were made of a variety of commerically available fibre types coated with nickel by a variety of techniques and heat-treated under various conditions. The results of this and previous studies are analysed with respect to a simple dissolution–reprecipitation model of the recrystallization process.

2. Experimental

2.1. Carbon fibres

The fibres chosen for examination are listed in Table I together with average values of their mechanical properties and diameters as measured in the authors' laboratory. Certain structural parameters of the fibres are included in Table II.

2.2. Nickel coatings

Bundles of the fibres, about 8 cm long, were coated with nickel with a variety of techniques: (i) Electroless deposition using a nickel acetate/hydrazine bath as described by Dini and Coronado [10], (ii) Electrolytic deposition from an aqueous nickel ammonium sulphate plating solution at 22° C, (iii) Deposition from nickel carbonyl vapour at 200° C in an argon carrier gas, (iv) Physical vapour deposition from molten nickel in a vacuum of $\sim 10^{-4}$ Pa. The thickness ranges and gas analyses of the coatings are shown in Table II. With the first three techniques it was possible to obtain coatings with a predetermined relatively even thickness throughout the bundle (see e.g. Fig. 4). The PVD coatings varied in thickness within the bundle because of shadowing. Reliable gas analysis of the coatings was difficult. Analyses of the electroless and carbonyl nickel were obtained from thick coatings deposited on glass. The analysis for the electroless nickel is in good agreement with that of Dini and Coronado [10]. The oxygen content of the electrolytic coatings was estimated by comparison of analyses from coated and uncoated fibres.

TABLE I Type and properties of fibres investigated (average values for at least 10 fibres).

Fibre and type	Average diameter (μm)	UTS ($MN m^{-2}$)	Young's Modulus ($GN m^{-2}$)
Modmor II HTS–PAN	9.5	2500	220
Courtauld HTS HTS–PAN	9.8	2300	210
Courtauld HM HM–PAN	8.7	1675	325
Modmor I HM–PAN	9.3	1520	330
Thornel 50 HM–Rayon	8.1	1550	350

TABLE II Types of nickel coatings deposited.

Coating	Range of Coating thickness (μm)	Analysis (wt %)		
		O	N	H
Electroless	0.5–5	0.17	0.18	0.01
Electrolyte on Modmor II	1–2	0.25	n.d.	n.d.
Electrolyte on Modmor I	1–2	0.45	n.d.	n.d.
Carbonyl	~0.1–5	0.28	n.d.	<0.01
PVD	up to 0.5	n.d.	n.d.	n.d.

2.3. Heat treatment

The bundle specimens were heat-treated at temperatures up to 1270° C. The majority of treatments were carried out with flowing argon of 99.995% purity in a conventional alumina-tube resistance furnace. The conditions of other treatments in hydrogen and vacuum are described in Section 3.1. The heat treatment temperature was measured to ±10° C with a Pt/Pt–10Rh thermocouple.

2.4. Investigation of fibre structure and properties

The fibres were investigated before and after heat-treatment by a variety of techniques:

(i) Both the axial tensile strength and Young's modulus were measured using a method similar to that described by Blakelock and Lovell [11]. The

properties of a given specimen bundle were measured as the average of ten individual fibres. For coated fibres, the measurements were made after removal of the coating by immersion in aqueous nitric acid/acetic acid solution [3], a treatment that had little affect on as-received fibres. Heavily degraded fibres with strengths below about $100\,MN\,m^{-2}$ were too fragile to be mounted for testing.

(ii) Samples from each specimen were mounted, sectioned and polished by standard techniques for metallographic examination. Scanning electron microscopy was used for the examination of fibre surfaces after removal of nickel.

(iii) The fibre structure was studied by means of X-ray diffraction using a Philips diffractometer. Co$K\alpha$ radiation was used to obtain the profile of the graphite (0 0 0 2) reflection from samples that had been lightly crushed to a powder. The width of the peak was used to estimate the crystallite size in the c-direction, L_c (i.e. the ribbon thickness), while the position of the peak maximum yielded the average (0 0 0 2) planar spacing [3]. During recrystallization the fibre structure is transformed to normal crystalline graphite with a relatively coarse crystallite size and consequently the (0 0 0 2) peak becomes sharp and is shifted to an angle corresponding to the normal graphite spacing [3]. Thus it was possible to estimate the degree of recrystallization in a given sample by comparison of the area under this peak and that under the peak corresponding to the remaining unrecrystallized fibre.

3. Results

3.1. Effects of heat-treatment atmosphere (excluding recrystallization effects).

Preliminary studies were made of the effect of heat-treatment atmosphere on Modmor II fibres with and without electroless nickel coatings. Treatments were carried out in the alumina-tube furnace with flowing argon or hydrogen of 99.995% purity and in a molybdenum-wound vacuum furnace in a vacuum of ~5 mPa.

The internal structure of uncoated fibres was unaffected by treatments of 1 h up to 1000° C. However, as shown in Fig. 1, the heat-treatment *in vacuo* caused significant weakening of the fibre, presumably due to surface attack. This is consistent with the conclusion of Barclay and Bonfield that fibres are weakened in a vacuum of this pressure at temperatures as low as 600° C [9].

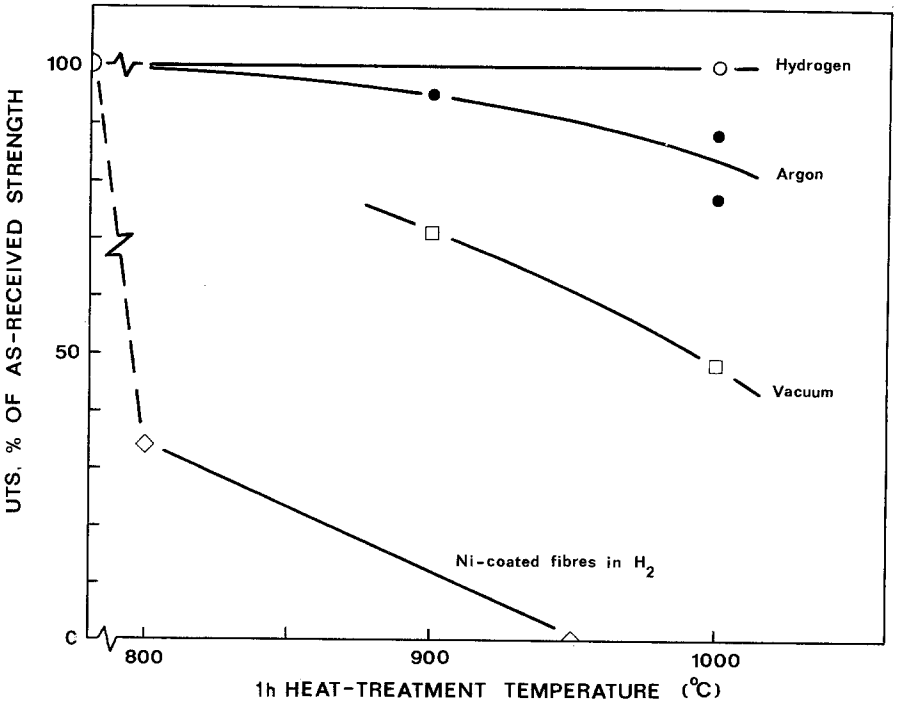

Figure 1 Effect of heat-treatment temperature and atmosphere on uncoated Modmor II fibres and on Ni-coated fibres in hydrogen.

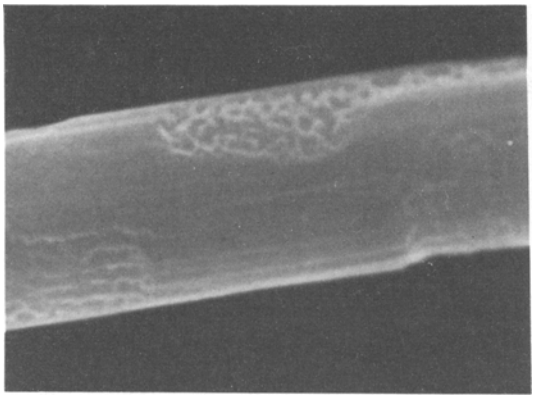

Figure 2 SEM picture showing surface attack of carbon fibre after heat-treatment in air-contaminated argon (nickel removed).

Similar treatments in argon caused some weakening while in hydrogen the fibres were unaffected (Fig. 1).

The behaviour of coated fibres was in complete contrast to the above. Both in argon and vacuum, the fibres were unaffected by up to 5 h treatments at temperatures up to that at which recrystallization began i.e. ~900° C (Section 3.2). Thus the nickel coating apparently provided protection against attack. In hydrogen, however, the fibres were severely weakened by surface attack after 1 h at 800° C, and at 950° C they had completely disappeared (Fig. 1). Thus nickel catalyses the reaction of hydrogen with the fibres presumably to form gaseous hydrocarbons.

No systematic, quantitative study was made of the effect of oxygen in the atmosphere. Nevertheless, it was observed that if insufficient care was taken to exclude air during the argon treatment a variable weakening of the fibres occured at temperatures as low as 700° C. This weakening was not associated with premature recrystallization, but was due to surface attack, an example of which is shown in Fig. 2.

3.2. Recrystallization; effects of fibre type and structure

The effects of 1 h heat-treatment temperature on the strength, elastic modulus and degree of recrystallization (measured by X-ray diffraction) of Modmor I, Modmor II and Thornel 50 fibres in electroless nickel are shown in Fig. 3.

The behaviour of Modmor II fibres was in agreement with that reported in earlier studies of HTS PAN-based fibres [3, 6]. Up to about 900° C

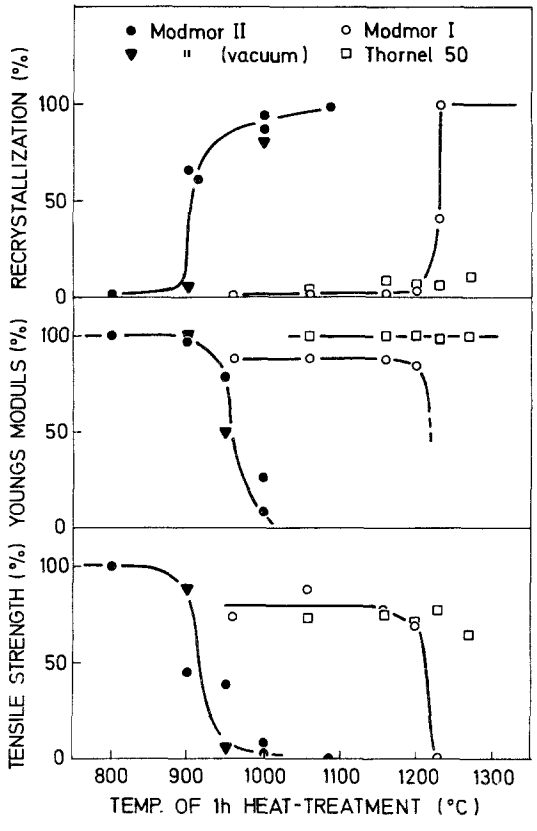

Figure 3 The effect of heat-treatment on the structure and properties of electroless nickel coated carbon fibres.

the fibres were unaffected, but above 900° C they rapidly recrystallized and suffered corresponding losses in strength and modulus. The progress of recrystallization could also be observed metallographically. Figure 4 to 6 demonstrate that the process proceeds from the surface to the centre of the fibre and is accompanied by the migration of bulk nickel to the centre, as observed by Shiota and Watanabe [6].

The HM fibres were far more stable. The Modmor I fibres did not exhibit rapid recrystallization until about 1230° C, while the Thornel 50 fibres did not recrystallize rapidly at 1270° C, the highest heat-treatment temperature. Unlike the type II fibres, both types of HM fibre exhibited small but measurable amounts of recrystallized graphite after treatments at temperatures as low as 1060° C (see Table IV). For convenience and for reasons to be made apparent in the discussion this recrystallization will be distinguished by the term "sub-critical". It was accompanied by a relatively small (10 to 20%) but consistent reduction in fibre

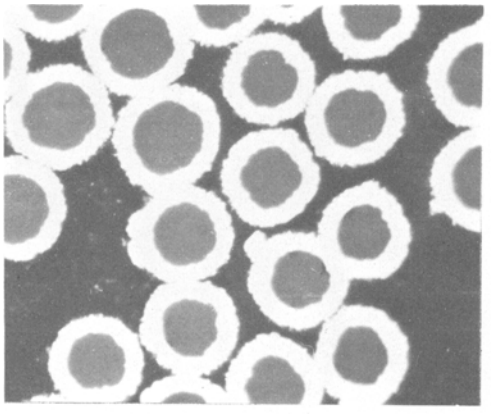

Figure 4 Modmor II fibres as-coated with electroless nickel.

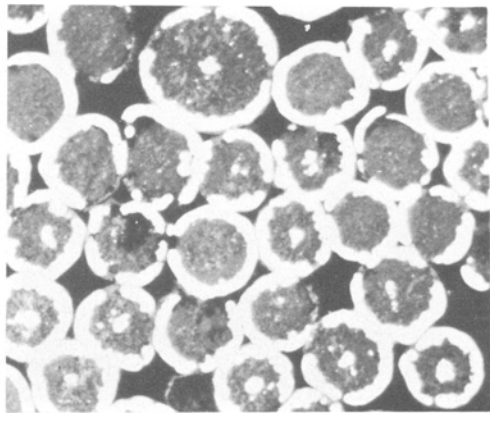

Figure 6 Electroless nickel coated Modmor II fibres after 1 h at 1000° C, fully recrystallized.

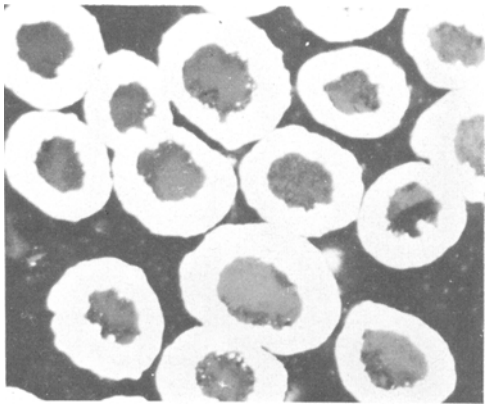

Figure 5 Electroless nickel coated Modmor II fibres after 1 h at 900° C, partially recrystallized.

strength. Similar small amounts of recrystallized graphite were observed in HM PAN fibres by Barnet *et al.* [4] with electron microscopy and similar reductions in the strength of Thornel 50 fibres well below the recrystallization temperature were observed by Sarian [5]. These effects are treated further in the discussion section.

The other fibre types, Courtaulds HTS and HM, coated with electroless nickel behaved in a similar manner to the above differing only in the temperature of rapid recrystallization. The recrystallization temperatures of the various fibres are given in Table III together with certain of their structural parameters. Values estimated from the results of Jackson and Marjoram [3] are also included. The

TABLE III Recrystallization temperature and structural parameters of carbon fibres.

Fibre	Ni–coating	Recrystallization temp. (°C) (i.e. temp. for 50% recryst. in 1 h)	Structural parameters of fibre		
			Crystallite size in *c*-direction L_c (nm)	(0 0 0 2) planar spacing *d* (nm)	Orientation of (0 0 0 2) planes. Av. angular deviation from axis from [17].
HTS PAN-base [3]	Electrolytic	~850	1.1 (3)	0.356 (3)	n.d.*
Modmor II	electroless	~900	1.6	0.351	23.5°
	electrolytic	~850	1.6	0.351	23.5°
	carbonyl	~850	1.6	0.351	23.5°
	PVD	~850	1.6	0.351	23.5°
Courtaulds HTS	electroless	~950	1.6	0.349	22.7°
Courtaulds HM	electroless	~1100	6.0	0.343	13.8°
HM PAN-base [3]	electrolytic	~1100	7.0 (3)	0.342 (3)	n.d.
Modmor I	electroless	1200–1230	7.25	0.341	7.8°
	electrolytic	1200–1230	7.25	0.341	7.8°
	carbonyl	1200–1230	7.25	0.341	7.8°
Thornel 50	electroless	>1270	5.25	0.341	8.1°
Thornel 50 [5]	electrolytic	1250 (100% within 24 h)	n.d.	n.d.	n.d.

*n.d. = not determined.

recrystallization temperature is here defined as that giving 50% recrystallization after 1 h. It is clear that a relationship exists between fibre stability and fibre structure and type. Thus the recrystallization temperature increases in the order HTS-PAN, HM-PAN, HM-Rayon and, more specifically, for the PAN-based fibres it increases with the structural order (increasing L_c and decreasing d (0 0 0 2)) and orientation. It is of interest to note that the same ranking of stability is observed with respect to oxidation [1, 12]. The results indicate that significant differences in stability may be observed for fibres of ostensibly the same type.

3.3. Recrystallization; effect of nickel coating

The heat-treatment studies were repeated with Modmor I and II fibres coated with the different types of nickel coating described in Section 2.2. Little difference in recrystallization behaviour was observed for the different coatings (Table III). With the electrolytic, carbonyl and PVD coatings the recrystallization temperature was reduced to about 850° C, as compared to 900° C for the electroless coating. Recalling Table I, this is possibly attributable to higher oxygen contents in the former.

The recrystallization did not appear to be affected significantly by the thickness of the coatings ($<0.2\,\mu$m) of carbonyl and PVD nickel were sufficient to produce normal recrystallization.

3.4. Recrystallization; effect of heat-treatment atmosphere

The majority of heat-treatments were in pure argon. In a vacuum of 5 mPa, Modmor II fibres exhibited very similar recrystallization behaviour to that in argon (Fig. 3).

As stated in Section 3.1, contamination of the argon by air did not affect the recrystallization of Modmor II fibres but led to reductions in fibre strength as a result of surface attack. In contrast to this, similar contamination caused a dramatic reduction in the recrystallization temperature of Modmor I fibres by as much as 200° C.

3.5. Isothermal studies

The above results refer mainly to isochronal studies, i.e. 1 h heat-treatments. For certain fibre/coating combinations isothermal studies were made for times of up to 5 h. These are introduced in the discussion section with reference to the model for the recrystallization process. Isothermal studies above and in the region of the recrystallization temperature were difficult because of the rapid and erratic nature of the process. For lower temperatures, at which the process is slow, reliance has been placed on the results of previous work [3, 5, 6].

4. Discussion

The precise nature of the recrystallization process of carbon fibres in nickel has not been established with certainty. Jackson and Marjoram [3] suggested that it occurs by the dissolution in nickel of carbon from the fibre followed by its reprecipitation as crystalline graphite. Warren and Wood [13] have argued that alternative processes activated by nickel atoms, but not involving dissolution in nickel, are also feasible. Here we have chosen to discuss the experimental results in terms of a simple dissolution–reprecipitation model which is presented in the Appendix. Briefly, it is postulated that the recrystallization occurs by the migration of a thin cylindrical ring of bulk nickel towards the centre of the fibre, dissolving carbon at its inner face and reprecipitating it at its outer face. This mechanism is suggested by the observations of this and previous studies [6].

Making the assumptions that: (i) the fibre structure is homogeneous and (ii) the thickness δ of the nickel does not change significantly during its migration, the following expression is obtained for the isothermal recrystallization rate:

$$V_u^{1/2} = V_0^{1/2} - Kt \quad (\text{for } t < V_0^{1/2}/K) \qquad (1)$$

where V_u is the volume of fibre remaining unrecrystallized at time t after the start of the process and V_0 is the original fibre volume. K is a rate constant and, if the process is controlled by the diffusion of carbon in nickel:

$$K = \pi^{1/2}\Omega D(C_f - C_0)/\delta \qquad (2)$$

for a fibre of unit length, where Ω is the molar volume of carbon, D the coefficient of diffusion of C in Ni, and C_0 and C_f the solubilities of carbon in nickel at equilibrium with crystalline graphite and the carbon fibre respectively. As is shown in the appendix, C_f is greater than C_0 to an extent dependent on the structural disorder of the fibre. Thus the value of $(C_f - C_0)$ reflects the driving force of the process.

According to Equation 1, a plot of isothermal recrystallization in the form $V_u^{1/2}$ versus t should

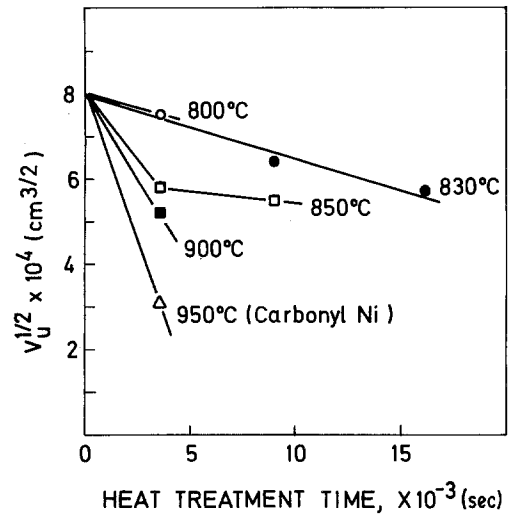

Figure 7 Recrystallization of Modmor II coated with PVD nickel. The $V_u^{1/2}$ scale refers to fibres of length 1 cm.

yield a straight line with slope $-K$. Fig. 7 shows such plots for the experimentally observed recrystallization of Modmor II fibres. The results are too few and exhibit too much scatter to provide a reliable test of the model but they can be used to provide a measure of the approximate relative recrystallization rates on the basis that $K = (V_0^{1/2} - V_u^{1/2})/t$ in cases of less than 100% recrystallization.

In Fig. 8, experimental recrystallization rates estimated in this way are compared with the predictions of the model (Equations 1 and 2) on an Arrhenius plot of log K versus $1/T$. Where sufficient information has been given, results of other studies have been included. For the model calculations, values of D and C were taken from [14] and [15] respectively. The value of δ was taken as 10^{-4} m and in calculating C_f from Equation A9 the values of L_c listed in Table III were used.

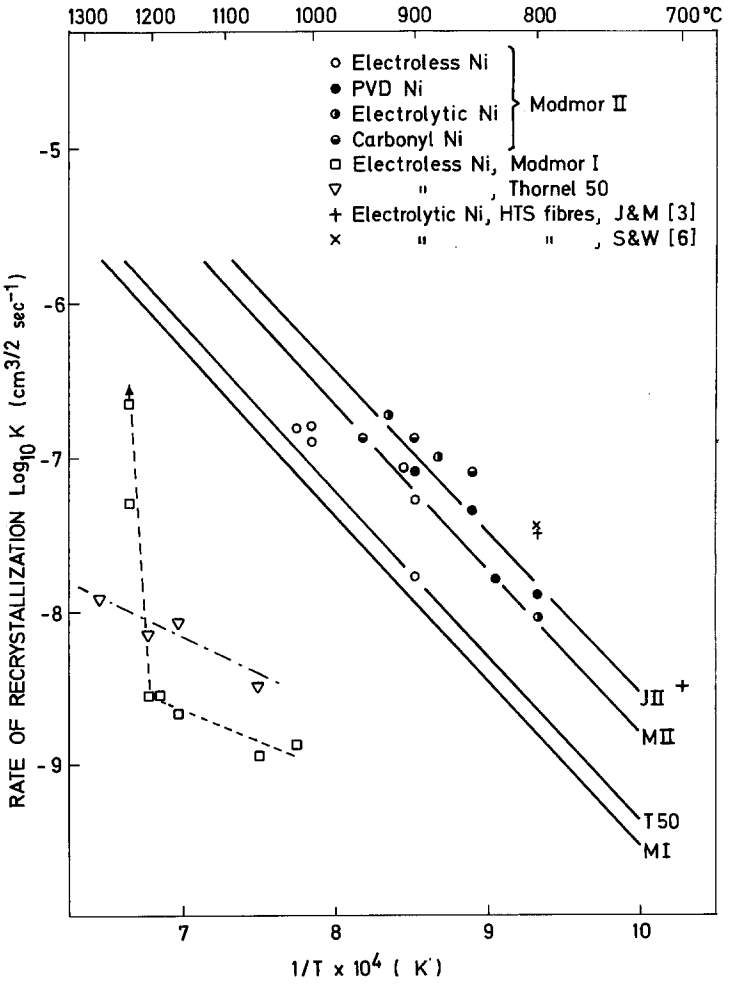

Figure 8 Experimental and predicted recrystallization rates of different types of C-fibres as a function of temperature. The full lines are the predictions for the following: MI = Modmor I, MII = Modmor II, T50 = Thornel 50, JII = the HTS fibres of [3].

The figure shows that, for HTS PAN-based fibres, there is reasonable agreement between experimental and predicted recrystallization rates in terms of both absolute values and, for a given fibre/Ni combination, the relative effect of temperature. The apparent activation energy of the process is approximately $240\,kJ\,mol^{-1}$; in terms of the model this is made up of the activation energy of the diffusion of carbon in nickel ($\sim 170\,kJ\,mol^{-1}$) plus a term corresponding to the effect of temperature on the solubility, C_0. It should be emphasized that the agreement between experiment and model does not constitute confirmation of the validity of the model but merely that the recrystallization behaviour is consistent with it.

The behaviour of HM fibres is not consistent with the model. In the temperature range of sub-critical recrystallization, the apparent recrystallization, rates are about two orders of magnitude lower than predicted. Thus the difference in recrystallization behaviour between HTS and HM fibres cannot be explained solely in terms of differences in the bulk structural order. However, for Modmor I fibres, the recrystallization rate rises sharply at their recrystallization temperature towards the predicted rate and similar behaviour is observed for the results from Courtauld HM fibres and the HM fibres of Jackson and Marjoram [3] when plotted in an analogous manner. Such behaviour is characteristic of a two-stage process, i.e. an initial incubation stage followed by the normal rapid recrystallization.

Barclay and Bonfield [9] identified an incubation stage prior to fibre dissolution, namely the wetting of the fibre surface by nickel. In the present case, i.e. recrystallization as opposed to dissolution, wetting is not considered to be a controlling factor, since the occurrence of the sub-critical recrystallization within 1 h of heat-treatment indicates that dissolution must have occurred. Furthermore, spheroidization of the nickel was not observed. An alternative explanation for the observed delay in recrystallization can be found from structural studies of HM fibres which indicate the presence of a sheath of highly oriented and ordered graphite at the fibre surface [16–18]. Such a surface sheath would exhibit an extremely low recrystallization rate and rapid recrystallization would not occur until it had been penetrated by nickel.

Penetration of the sheath could occur partly by normal, equilibrium dissolution of the carbon in nickel and partly by very slow recrystallization. The extent of the first of these is limited by the solubility of carbon in nickel. Simple diffusion calculations show that above about 1000° C the nickel coating would be saturated with carbon in less than 1 h. When this dissolution is insufficient to remove the protective sheath, further penetration would have to occur by slow recrystallization and an incubation time would be observed. At a sufficiently high temperature dissolution would be sufficient to remove the stable sheath almost completely and very rapid recrystallization would occur. On the basis of this interpretation, the observed differences in recrystallization temperature of the different HM fibres can be attributed to differences in thickness and/or stability of the sheath. Similarly the reduction in recrystallization temperature caused by contamination of the heat-treatment atmosphere is explained by a premature destruction of the sheath by oxidation.

The above interpretation also implies that the sub-critical recrystallization occurring below the recrystallization temperature is not true recrystallization but is mainly due to dissolved carbon reprecipitating as graphite during cooling. Support for this is provided by Table IV which compares the observed values of sub-critical recrystallization with the amounts of dissolved graphite predicted on the basis of equilibrium solubilities and the thickness of the coating. The moderate losses of fibre strength observed in the sub-critical temperature range may to some extent be associated with this dissolution, and it is to be noted that the strength losses observed in Thornel 50 fibres by Sarian [5] occurred mainly within the first hour and were relatively small thereafter for treatments of up to 2000 h. Nevertheless, that some true recrystallization occurs in the sub-critical region is indicated by the study of Jackson and Marjoram [3] in which HM fibres eventually recrystallized after prolonged annealing below the temperature of rapid recrystallization.

The value of sub-critical recrystallization just below the recrystallization temperature can be used to obtain an estimate of the effective thickness of the stable sheath. The values ~ 4 vol % and > 11 vol % for Modmor I and Thornel 50 fibres respectively (Table IV) lead to estimated sheath

TABLE IV Predicted carbon concentrations in nickel coatings on HM fibres compared with observed recrystallized graphite.

Fibre	Coating thickness, μm (and vol. fraction)	Heat treatment temp. (°C)	Predicted fraction of fibre dissolved (vol%)	Apparent recrystallization observed (vol%)
Modmor I (calculation based on 9.3 μm diameter)	1–2 (0.3–0.5)	960	0.5–1.5	0
		1060	0.8–2	1–1.5
		1160	1–2.4	2–2.5
		1190	1.1–2.5	2.5
		1200	1.2–2.6	2–3
Thornel 50 (calculation based on 8 μm diameter)	~4 (~0.75)	1060	5.5	3
		1160	7.0	7.5
		1200	8.0	6
		1230	8.5	6
		1270	10	11

thickness of ~0.1 and >0.25 μm for these fibres. These values are in reasonable agreement with the structural investigations mentioned above [17, 18] which indicate a value of ~1 μm.

5. Conclusions

The recrystallization behaviour of carbon fibres in the presence of nickel is sensitive to the fibre type; the temperature of rapid recrystallization increases in the order: PAN-based HTS fibres, PAN-based HM fibres, rayon-based HM fibres. Furthermore, for PAN-based fibres the fibre stability increases with, for example, decreasing basal plane spacing, increasing crystallite size and increasing axial orientation of the basal planes.

The recrystallization behaviour of HTS PAN fibres is consistent with a dissolution–reprecipitation process controlled by the diffusion of carbon in nickel. The delayed recrystallization of HM fibres cannot be explained in terms of this model alone but is consistent with the existence of a very stable surface sheath having a thickness of about 0.1 to 0.25 μm. The observed relationship between the stability and the bulk structural properties of PAN-based fibres is therefore probably indirect.

Nickel-coated carbon fibres are extremely sensitive to chemical attack by oxygen and hydrogen at temperatures well below the normal recrystallization temperature. Furthermore, a small proportion of oxygen in the heat-treatment atmosphere reduces the recrystallization temperature of Modmor I fibres by as much as 200° C.

The recrystallization behaviour of carbon fibres is not significantly affected by the purity of the nickel coating, at least within the range of purity existing in the present investigation. In systems of higher purity the question of the relative importance of purity and fibre structure remains open.

The above conclusions indicate that the problem of fibre recrystallization in C-fibre/nickel composites at elevated temperatures can to some extent be overcome by the choice of fibres with a suitable structure. The problem of fibre degradation by the attack of gaseous species such as oxygen and hydrogen presents a more serious problem. The attack of the fibres could possibly by avoided by the use of suitable nickel alloy matrices. The fabrication of composites with alloy matrices, however, presents considerable practical difficulties and also introduces the possibility of reactions between fibre and alloying elements. A more practical solution may be the development of suitable protective coatings for composites with pure nickel matrix.

6. Appendix

Fig. 9a illustrates the proposed model of recrystallization for a fibre in cross-section. A cylindrical ring of nickel migrates towards the centre of the fibre, dissolving carbon from the fibre on its inside face and reprecipitating it as crystalline graphite on its outer surface. Fig. 9b illustrates schematically the carbon concentration across the nickel ring. C_f is the solubility of carbon in nickel in equilibrium with the fibre while C_0 is the solubility in equilibrium with crystalline graphite. C_f is greater than C_0 to an extent dependent on the excess structural energy of the fibre. C' is the concentration of carbon in the nickel at the fibre surface; this can be less than C_f if the diffusion of carbon away from the interface is faster than its

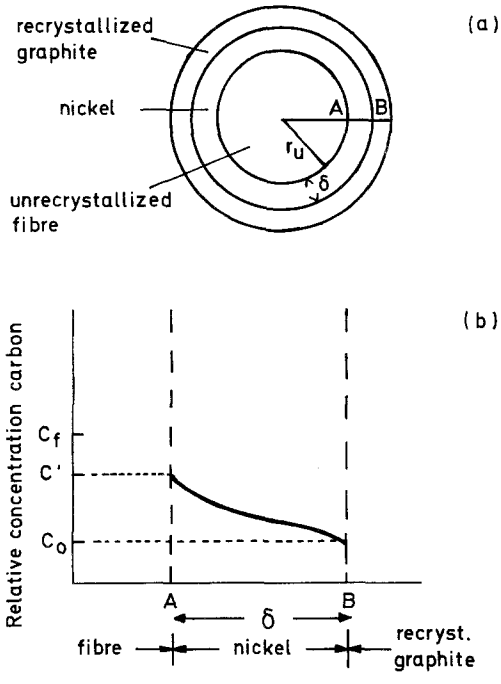

Figure 9 Schematic illustration of recrystallization model. (a) fibre cross-section (b) carbon concentration profile across nickel ring.

dissolution. It is assumed that the rate of precipitation of crystalline graphite is sufficient to maintain the carbon concentration at the nickel/graphite interface at C_0.

With these conditions the rate of dissolution of the unrecrystallized part of the fibre is proportional to its surface area, i.e. for unit length of fibre

$$-\frac{dV_u}{dt} = 2\pi r_u \Omega k (C_f - C'), \qquad (A1)$$

where V_u is the volume of fibre remaining unrecrystallized, Ω is the molar volume of carbon and k is the rate constant for the dissolution process.

Similarly the volume of carbon diffusing across the nickel layer:

$$\frac{dV}{dt} = 2\pi r_u \Omega \, [D (C' - C_0)/\chi] \qquad (A2)$$

where D is the coefficient of diffusion of carbon in nickel. $(C' - C_0)/\chi$ is the concentration gradient across the ring and so χ is an effective diffusion distance which will be set approximately equal to the width of the ring i.e. $\chi \approx \delta$.

When a steady state is attained the rate of carbon dissolution and carbon diffusion will be equal i.e. $dV_u/dt = dV/dt$. Equating Equations A1 and A2 and eliminating C' yields:

$$-\frac{dV_u}{dt} = 2\pi r_u \Omega \frac{kD(C_f - C_0)}{k\delta + D} \qquad (A3)$$

When $D \gg k\delta$ this becomes

$$-\frac{dV_u}{dt} \approx 2\pi r_u \Omega k (C_f - C_0) \qquad (A4)$$

and the process can be said to be controlled by the rate of dissolution. Similarly when $k\delta \gg D$

$$-\frac{dV_u}{dt} \approx 2\pi r_u \Omega D (C_f - C_0)/\delta \qquad (A5)$$

and the process is controlled by the diffusion of carbon in nickel.

Putting $r_u = (V_u/\pi)^{1/2}$, for unit length of fibre, Equations A4 and A5 can be integrated to obtain V_u as a function of t

$$V_u^{1/2} = V_0^{1/2} - Kt \qquad (A6)$$

where V_0 is the original volume of the fibre per unit length and, for the diffusion controlled process:

$$K = \pi^{1/2} \Omega D (C_f - C_0)/\delta \qquad (A7)$$

It is to be noted that it has here been assumed that both C_f and δ are constant i.e. independent of V_u. The assumption that C_f is constant implies that the fibre is structurally homogeneous. Were the volume of the nickel ring to remain constant then clearly the width δ would increase as V_u decreased i.e. as the ring migrated inwards. However, it is observed experimentally that small amounts of nickel are left behind as the ring advances and therefore δ can be considered to remain relatively constant.

To estimate the value of C_f it is assumed that the structure of the fibres is made up of square-sectioned ribbon-like crystallites of infinite length and of width, L_c, the crystallite size in the c-direction measured by X-ray line broadening. The excess internal energy of the fibres is then considered to be the energy of the crystallite boundaries. Thus the energy per unit volume:

$$E = \tfrac{1}{2} 4 L_c \gamma / L_c^2 = \frac{2\gamma}{L_c} \qquad (A8)$$

where γ is the crystallite boundary free energy per unit area. The factor $\frac{1}{2}$ arises because each boundary is shared by two crystallites. A similar calcu-

lation for the coarse recrystallized graphite ($L_c \approx 100\,\text{nm}$) yields a relatively negligible value for its internal energy. Thus the difference in molar free energy, ΔE, between fibre and recrystallized graphite is given by:

$$\Delta E \approx \frac{2\Omega\gamma}{L_c}$$

Since $E = RT\ln a_f/a_0$, where a_f and a_0 are the activities of carbon in the fibre and graphite respectively, then

$$\ln a_f/a_0 = \frac{2\Omega\gamma}{RTL_c},$$

and, assuming that solubilities are proportional to the activities,

$$C_f = C_0 \exp 2\Omega\gamma/RTL_c. \qquad \text{(A9)}$$

Thus C_f can be obtained in terms of C_0. For example, for an HTS fibre with $L_c = 1.6\,\text{nm}$, taking γ as $0.5\,\text{J/m}^{-2}$ and T as 1173 K, Equation A9 gives $C_f = 1.47\,C_0$. Similarly, for an HM fibre with $L_c = 7\,\text{nm}$, $C_f = 1.09\,C_0$.

Acknowledgements

This work was supported by the Swedish Board of Technical Development (STU). The authors also thanks J. Almström, H. Damberg and S. Larsson for experimental assistance, S. Carlsson and S. Gunnarsson of Linköping University of Technology for supplies of electrolytically-coated fibres, and Professor H. Fischmeister for valuable discussions and encouragement.

References

1. F. S. GALASSO and J. PINTO, *Fibre Sci. Tech.* **2** (1970) 303.
2. D. M. BRADDICK, P. W. JACKSON and P. J. WALKER, *J. Mater. Sci.* **6** (1971) 419.
3. P. W. JACKSON and J. R. MARJORAM, *ibid.* **5** (1970) 9.
4. S. V. BARNETT, S. J. HARRIS and J. F WEAVER, *Faraday Special Discussions of the Chem. Soc.*, No. 2 (1972) 144.
5. S. SARIAN, *J. Mater. Sci.* 8 (1973) 251.
6. I. SHIOTA and O. WATANABE, *J. Jap. Inst. Metals* 38 (1974) 794.
7. P. J. GOODHEW, A. J. CLARKE and J. E. BAILEY, *Mater. Sci. Eng.* 17 (1975) 3.
8. R. WARREN and M. CARLSSON, "Proceedings of the V International Conference on Chemical Vapour Deposition", edited by Blocher and Hintermann (The Electrochem. Soc., Princeton N. J., 1975) p. 611.
9. R. B. BARCLAY and W. BONFIELD, *J. Mater. Sci.* 6 (1971) 1076.
10. J. W. DINI and P. R. CORONADO, *Plating* **54** (1967) 385.
11. H. D. BLAKELOCK and D. R. LOVELL, 24th Annual Technical Conference on Reinforced Plastics/Composites Division, Section 6-B (Soc. Plastics Ind., Inc. USA, 1969) p. 1.
12. D. J. THORNE and A. J. PRICE, *Fibre Sci. Tech.* 4 (1971) 9.
13. R. WARREN and J. WOOD, "Reactivity of Solids" edited by J. Wood, O. Lindqvist, C. Helgesson and N. G. Vannerberg, (Plenum, London and New York, 1977) p. 779.
14. J. J. LANDER, H. E. KERN and A. L. BEACH, *J. Appl. Phys.* **23** (1952) 1305.
15. W. B. DUNN, R. B. McLELLAN and W. A. OATES, *Trans. AIME* **242** (1968) 2129.
16. F. TUINSTRA and J. L. KOENIG, *J. Composite Mater.* 4 (1970) 492.
17. R. J. DIEFENDORF and E. W. TOKARSKY, AFML-TR-72-133, parts I and II.
18. B. J. WICKS and R. A. COYLE, *J. Mater. Sci.* **11** (1976) 376.

Received 31 March and accepted 28 April 1977.